The EMBO Journal (2008) 27, 1995–2005 | © 2008 European Molecular Biology Organization | All Rights Reserved 0261-4189/08
www.embojournal.org

THE EMBO JOURNAL

Novel type of Ras effector interaction established between tumour suppressor NORE1A and Ras switch II

Benjamin Stieglitz[1,4], Christine Bee[1], Daniel Schwarz[1], Özkan Yildiz[2], Anna Moshnikova[3], Andrei Khokhlatchev[3] and Christian Herrmann[1,*]

[1]Physikalische Chemie 1, Fakultät für Chemie und Biochemie, Ruhr-Universität Bochum, Bochum, Germany, [2]Max-Planck-Institut für Biophysik, Abteilung Strukturelle Biologie, Frankfurt, Germany and [3]Department of Pathology, University of Virginia Health Science Center, Charlottesville, VA, USA

A class of putative Ras effectors called Ras association domain family (RASSF) represents non-enzymatic adaptors that were shown to be important in tumour suppression. RASSF5, a member of this family, exists in two splice variants known as NORE1A and RAPL. Both of them are involved in distinct cellular pathways triggered by Ras and Rap, respectively. Here we describe the crystal structure of Ras in complex with the Ras binding domain (RBD) of NORE1A/RAPL. All Ras effectors share a common topology in their RBD creating an interface with the switch I region of Ras, whereas NORE1A/RAPL RBD reveals additional structural elements forming a unique Ras switch II binding site. Consequently, the contact area of NORE1A is extended as compared with other Ras effectors. We demonstrate that the enlarged interface provides a rationale for an exceptionally long lifetime of the complex. This is a specific attribute characterizing the effector function of NORE1A/RAPL as adaptors, in contrast to classical enzymatic effectors such as Raf, RalGDS or PI3K, which are known to form highly dynamic short-lived complexes with Ras.

The EMBO Journal (2008) **27,** 1995–2005. doi:10.1038/emboj.2008.125; Published online 3 July 2008
Subject Categories: signal transduction; structural biology
Keywords: adaptor; apoptosis; interface; lifetime; protein interaction

Introduction

The members of the superfamily of small GTP binding proteins stimulate a variety of vital cellular responses in a nucleotide-dependent manner. The exchange of the bound nucleotide GDP for GTP is accompanied by conformational rearrangements of switch I and switch II regions (Vetter and Wittinghofer, 2001). Ras is enabled to form a complex with downstream effector proteins, which subsequently provoke crucial cellular functions such as transcription, cell-cycle progression and cytoskeletal rearrangements only in the GTP-bound conformation. Structural characterizations of different effectors in complex with Ras have revealed a protein domain common to all Ras effectors and this domain is responsible for interaction with the members of the Ras family. This binding module known as Ras binding domain (RBD) or Ras association domain (RA) consists of about 80–100 amino acids whose tertiary structure corresponds to the folding topology of ubiquitin. Interaction with Ras is established by formation of an anti-parallel intermolecular β-sheet between switch I of Ras and strand β_2 of the canonical ubiquitin fold (Herrmann, 2003). As a result of these common structural features, the affinities and dynamic properties of the Ras/effector complexes are markedly similar. Quantitative binding studies have demonstrated that they form short-lived complexes with K_D values in the range of 20 nM–2 μM (Wohlgemuth *et al*, 2005).

In general, Ras effector proteins are enzymes that initiate intracellular signalling that typically leads to cell growth and proliferation (Malumbres and Barbacid, 2003). By contrast, a new class of effector proteins that participate rather in growth and tumour suppressive pathways has been discovered (van der Weyden and Adams, 2007). This class, called Ras association domain family (RASSF), is encoded by six genes, each of them being expressed in multiple splice variants. RASSF proteins have been reported to interact with Ras by means of a putative RBD located in a highly conserved C-terminal region of all RASSF members (Dammann *et al*, 2000; Agathanggelou *et al*, 2005). Over the past years, RASSF proteins have been the subject of intensive investigations as it turned out that they are frequently downregulated by promoter methylation during cancer development. In fact, epigenetic inactivation of RASSF members such as RASSF1A is one of the most common events observed in carcinogenesis (Pfeifer *et al*, 2002; Agathanggelou *et al*, 2005). It has been shown that ectopic expression of RASSF proteins in several cancer cell lines lacking the respective endogenous transcripts inhibits cell growth and tumorigenicity (Dammann *et al*, 2003; Aoyama *et al*, 2004). The molecular mechanisms by which RASSF proteins induce growth and tumour suppression are not determined yet. Several reports indicate that members of the RASSF modulate microtubule dynamics in mitosis and hence maintain genomic stability (Liu *et al*, 2003, 2005; Moshnikova *et al*, 2006). Other studies have demonstrated that RASSF proteins can promote apoptosis by interacting by means of a putative coiled-coil region known as SARAH domain with proapoptotic proteins such as MST1/2 and MOAP-1 (Khokhlatchev *et al*, 2002; Scheel and Hofmann,

*Corresponding author. Physikalische Chemie I, Ruhr-Universität Bochum, Arbeitsgruppe Protein-Interaktionen, Fakultät für Chemie, Universitätsstrasse 150, 44780 Bochum, Germany.
Tel.: +49 0234 322 4173; Fax: +49 0234 321 4785;
E-mail: chr.herrmann@rub.de
[4]Present address: MRC National Institute for Medical Research, The Ridgeway, Mill Hill, London NW7 1AA, UK

Received: 5 March 2008; accepted: 4 June 2008; published online: 3 July 2008

2003; Praskova *et al*, 2004; Baksh *et al*, 2005; Oh *et al*, 2006; Vos *et al*, 2006). Unlike the classical Ras effectors, RASSF proteins lack any catalytic activity. Rather, they function as adaptor proteins that are capable of assembling and regulating other signalling components. However, the role of Ras or Ras-like GTPases in the regulation of growth and tumour suppressive activities of RASSF proteins remains unclear.

Most evidence for the interaction of RASSF members with Ras exists for the founding member RASSF5, primordially named NORE1A (Novel Ras Effector 1A) whose gene encodes two splice variants. NORE1A binds Ras with high affinity *in vivo* and *in vitro* and shares the growth and tumour suppressive properties with other RASSF members such as RASSF1A (Vavvas *et al*, 1998; Vos *et al*, 2003; Wohlgemuth *et al*, 2005). In contrast, the shorter splice variant RAPL (Regulator of Adhesion and Polarization enriched in Lymphocytes), preferentially expressed in T cells, forms a complex with Rap1 and mediates the spatial distribution of the integrin LFA-1 (Katagiri *et al*, 2003; Kinashi and Katagiri, 2004; Price and Bos, 2004; Miertzschke *et al*, 2007). To gain structural insights into complex formation of small GTP binding proteins and effectors of the RASSF, we solved the crystal structure of Ras bound to the RBD of NORE1A/RAPL. The structure reveals a novel type of Ras interaction with its effectors, which, as our biochemical analysis suggests, is well suited for the adaptor-type functions of the RASSF proteins.

Results

Molecular recognition of NORE1A by Ras

The RA of NORE1A is predicted by SMART (Schultz *et al*, 1998; Letunic *et al*, 2006) to cover residues 272–364 in the human sequence with a size of 92 amino acids common for Ras effectors. Experiments in transfected HEK293 cells revealed that the predicted RA is incapable of interacting with Ras. As shown in Figure 1, the NORE1A construct 254–416 comprising the RA and the C-terminal SARAH domain is not sufficient for Ras binding. Similarly, the construct 119–268, which contains the C1 domain and the flanking region of the predicted RA domain, is also deficient in Ras binding (Figure 1). These findings led us to conclude that the minimal fragment capable of interacting with Ras consists of an overlapping region of both constructs. Therefore, we established a construct that covers the predicted RA domain and extends by 68 residues towards the N terminus. This 160-amino-acid construct clearly interacts with Ras in transfected HEK293 cells (Figure 1). Interestingly, a similar fragment of murine NORE1A (residues 200–358) has been reported to bind to Ras with high affinity (Wohlgemuth *et al*, 2005) *in vitro*. Apart from five amino acids, the human NORE1A and murine NORE1A are identical within this range.

To understand how NORE1A is recognized by Ras on a molecular basis, we attempted to crystallize the 160-amino-acid comprising construct of murine NORE1A in complex with Ras. The Ras isoform we used is H-Ras ending at residue 166, as previous work has shown that the flexible C terminus of Ras renders the full-length protein unsuitable for crystallization (Vetter and Wittinghofer, 2001). As co-crystallization of wild-type (wt) proteins was not successful, we used the NORE1A mutant K302D and the Ras double mutant D30E/E31K because this strategy was also helpful in the crystallization of other Ras/effector complexes (Nassar *et al*, 1996; Vetter *et al*, 1999). This double mutant of Ras carries the Rap1 residues in these two positions of switch I (Terada *et al*, 1999) whereas mutation of K302D in NORE1A was reported to decrease the specificity for Ras and Rap1 (Wohlgemuth *et al*, 2005).

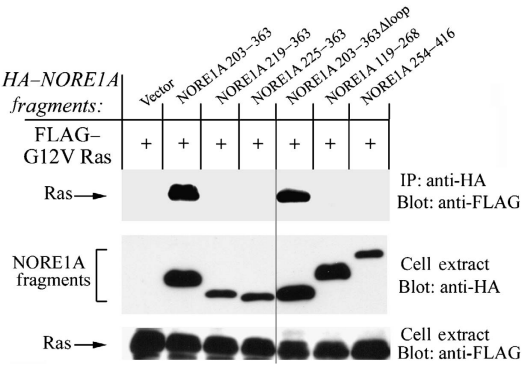

Figure 1 Interaction of wt and mutant NORE1A protein fragments with H-Ras *in vivo*. HEK293 cells were transfected with HA-tagged fragments of NORE1A and FLAG-tagged full-length G12V H-Ras as indicated. Cell lysates were precipitated for HA and the precipitates were probed with antibody against FLAG (upper panel) by western blotting. Middle and lower panels show expression of HA-tagged and FLAG-tagged proteins in cell extracts. A non-relevant lane was removed from all panels during the creation of this figure; the position where images were combined is indicated by a vertical black line.

The three-dimensional structure of the complex was solved at 1.8 Å resolution (Table I and Supplementary Figure 1). The current model covers all residues of the Ras molecule bound to the nucleotide GppNHp as well as the magnesium ion and NORE1A residues 200–248 and 274–357. The structure of the Ras–NORE1A complex reveals that NORE1A has a ubiquitin fold similar to RBDs of other effectors (Figure 2A and B) but it is remarkably extended by an insertion between β_1 and β_2 and an N-terminal elongation as described below. Residues 230–358 of NORE1A cover a mixed five-stranded β-sheet with two flanking α-helical regions and one additional 3_{10}-helix forming the ubiquitin α/β-roll. This structural segment exhibits a similar protein–protein interaction pattern with Ras as seen before in other Ras effector complex structures with an interprotein β-sheet formed between the switch I region of Ras and strand β_2 within the ubiquitin fold of NORE1A. Comparison with previously solved RBD structures reveals a large extension of strands β_1 and β_2 causing an intimate interplay between 10 residues of switch I of Ras and 5 residues of β_2 of NORE1A (Figures 2B, 3A and C, and Supplementary Figure 2).

There is no electron density for residues 249–273 of NORE1A, which form most likely a flexible loop, connecting strands β_1 and β_2. However, this part is dispensable for complex formation, as a deletion of this segment does not affect the interaction with Ras in HEK293 cells (Figure 1). We could quantify this result using the guanine nucleotide dissociation inhibitor (GDI) assay mentioned below. The NORE1A deletion mutant (255–274) binds Ras with the same affinity as the wt protein (see below).

The N-terminal residues 200–230 of NORE1A form a helix α_N and a short strand β_N, which are connected by a type I reverse turn. This N-terminal extension is tightly packed against the ubiquitin fold (Figure 2A) predominantly through hydrophobic interactions with strand β_1 and helix α_2. No counterpart has been observed for this additional structural

Table I Crystallographic statistics for the Ras/NORE1A complex

Data collection		Refinement	
Space group	C_2	Resolution range (Å)[a]	10–1.8
Unit cell		R_{work} (%)[b]	19.3
a (Å)	79.6	R_{free} (%)[c]	23.0
b (Å)	88.0	Number of atoms	
c (Å)	56.5	Protein	2396
β (deg)	125.0	GppNHp/Mg^{2+}	32/1
X-ray source	ESRF ID14-4	Number of water molecules	115
Wavelength (Å)	0.933	Average *B* factor (Å^2)	25.8
Resolution range (Å)[a]	10–1.78 (1.85–1.78)	RMS deviations from ideal values	
Number of total reflections	30 212	Bond lengths (Å)	0.015
Number of unique reflections	29 894	Bond angles (deg)	1.456
Completeness (%)[a]	97.2 (86.3)	Ramachandran plot	
I/σ[a]	13.6 (4.1)	Residues in most favoured regions (%)	94.4
R_{merge} (%)[a,d]	8.6 (34.8)	Residues in additional allowed regions (%)	5.6

[a]Values in parentheses correspond to the highest resolution shell.
[b]$R_{work} = \sum_{hkl}|F_o - F_c|/\sum_{hkl}|F_o|$, where F_o and F_c are the observed and calculated structure factors, respectively.
[c]$R_{free} = \sum_{hkl}|F_o - F_c|/\sum_{hkl}|F_o|$ was calculated with 5% of the data omitted from structure refinement.
[d]$R_{merge}(I) = \sum_{hkl}\sum_i|I_{hkl,i} - \langle I_{hkl}\rangle|/\sum_{hkl}\sum_i I_{hkl,i}|$, where $\langle I_{hkl}\rangle$ is the average intensity of the multiple $I_{hkl,i}$ observations for symmetry-related reflections.

element among the characterized Ras effector complexes. Most strikingly, residues C220 and L221 of the reverse turn form a hydrophobic interface with M67 and Y64 of switch II of Ras (Figure 3D and Supplementary Figure 2). This interface extends under participation of I36 of switch I and F234 of β_1 of NORE1A. To study the significance of this unique switch II binding site, we created two N-terminal deletions in the human variant of NORE1A 203–363 lacking the first 16 and 25 residues, respectively, and investigated the interaction with Ras in HEK293 cells. Remarkably, even the minimal deletion of amino acids 203–219, which comprise the helix α_N, completely abolished the interaction of NORE1A with Ras (Figure 1). These results clearly show that the N-terminal extension of NORE1A is essential for the interaction with Ras.

Mutational analysis of the interface

To analyse the quantitative contribution of amino acids participating in intermolecular interactions, and in particular to address the importance of switch II contacts, we created point mutants within the binding interface of NORE1A-RBD. The interaction between Ras and NORE1A was analysed by the GDI assay, which was used earlier for other Ras effectors. This method is based on the inhibition of guanine nucleotide dissociation by effector binding (Figure 4A) (Herrmann *et al*, 1996). We obtained an equilibrium dissociation constant K_D for the NORE1A–Ras complex of 0.08 μM. This value is comparable with the Ras–Raf interaction, which was found to have the highest affinity among all Ras effectors characterized so far (Figure 4B). The K_D value determined for Rap1 is 1.3 μM, indicating a clear preference of NORE1A to interact with Ras (Figure 4D). As mentioned above, we use the Ras mutant D30E/E31K for co-crystallization. This mutant mimics the effector binding site of Rap1, as the switch I regions of Ras and Rap1 differ only in these two residues. According to this, we obtained a K_D of 1.23 μM for Ras D30E/E31K, which is nearly the same as for wt Rap1 (Table II). On the other hand, the reverse mutation E30D/K31E in Rap1 shows a dissociation constant of 0.2 μM, which is in the range of that of wt Ras. The mutation K302D in NORE1A represents a charge reversal that diminishes the discrimination between Ras and Rap1 as can be seen by the similar K_D values of 0.71 and 0.69 μM for the complexes of this mutant with Ras and Rap1, respectively. The pair Ras D30E/E31K and NORE1A K302D, which we have used for crystallization, shows a K_D value of 0.77 μM. Although these data clearly suggest a salt bridge swapping between the mutant pair Ras(D30E/E31K)–NORE1A(K302D) and the corresponding wt proteins, we cannot observe this scenario in our structure, as both residues, aspartate 302 of the NORE1A mutant and lysine 31 of the Ras mutant, create polar contacts to a symmetry-related molecule (Supplementary Figure 3).

Residues of NORE1A involved in side-chain contacts within the intermolecular β-sheet of the two proteins were mutated to alanine. As mentioned above, β_2 of NORE1A is the major contact point to switch I of Ras. Our analysis indicates K283 from β_2 as the most essential residue that creates a salt bridge with D38 and two water-mediated contacts with D33 and P34 of Ras (Figure 3A and C). The loss of the lysine side chain perturbs Ras binding to a large extent, resulting in a 240-fold decrease in affinity (Table III). Mutation of D280 and Q284 of β_2 to Ala has only a weak effect on Ras binding. Apart from K283, another lysine (K303) at the edge of helix α_1 forms a crucial interaction with Asp33 of Ras (Figure 3C and Supplementary Figure 2). Mutation of K303 to Ala leads to a 35-fold reduction in binding affinity to Ras. There is no direct polar interaction between β_1 strand of NORE1A and switch I of Ras. Glu37 of Ras makes a water-mediated contact to K236 in the β_1 of NORE1A, which has only a modest contribution to the interaction with Ras. Adjacent to K236, the side chain of F234 is involved in the hydrophobic switch II interface formed between C220 and L221 of the N-terminal reverse turn in NORE1A and Y64, M67 of Ras switch II and I36 of Ras switch I (Figure 3D). Confirming our structural findings, single mutations of F234, C220 and L221 of NORE1A to alanine weaken the affinity 5- to 20-fold (Table III). As the mutants C220A and L221A of NORE1A might be still capable of contributing to hydrophobic interactions with Ras switch II, we also generated the Asp mutations C220D and L221D. The introduction of a negative charge at these positions should impair the hydrophobic network with Ras switch II to a much stronger extent than corresponding Ala mutations. In agreement with this, we obtained binding affinities that

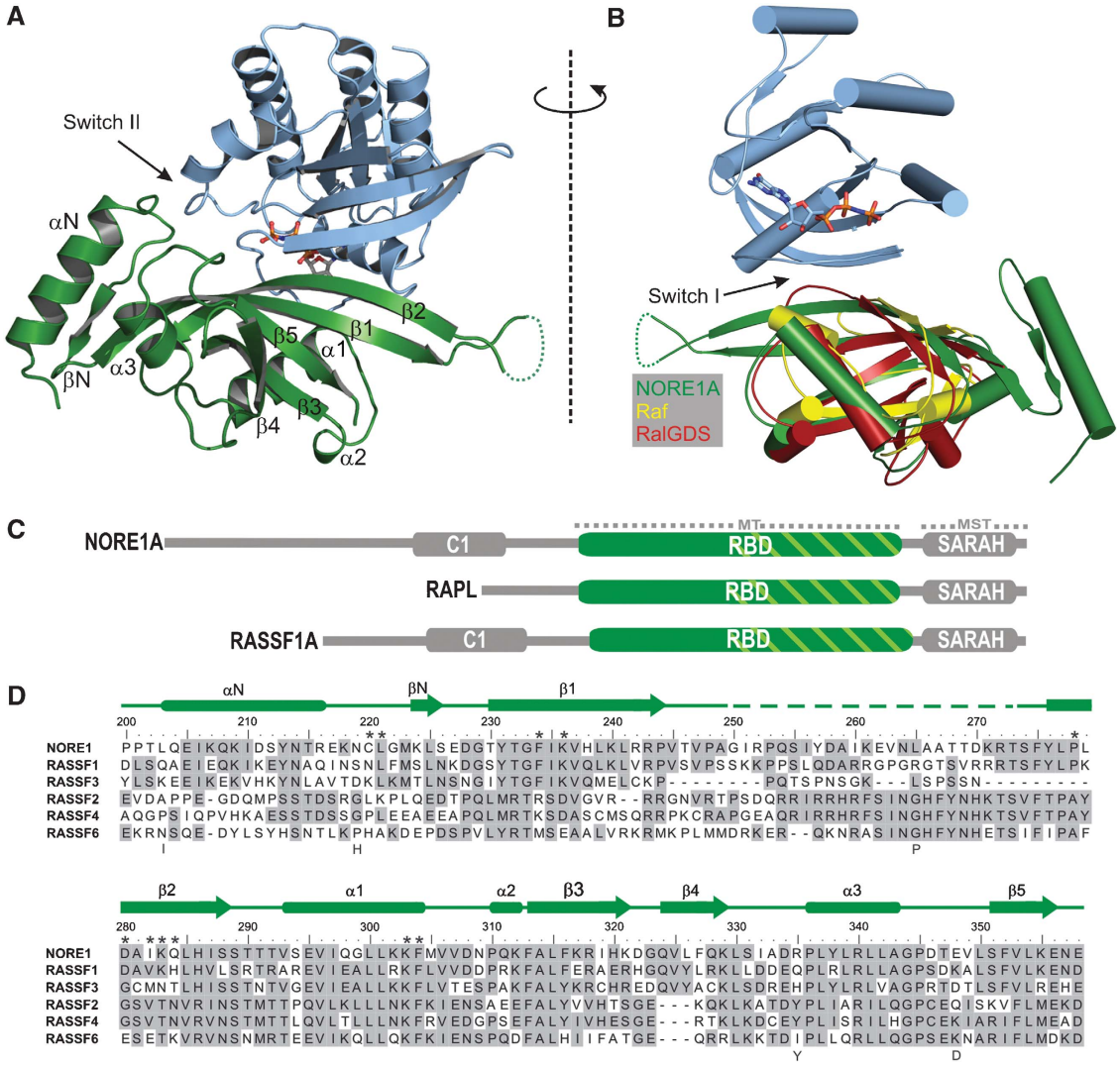

Figure 2 Crystal structure of the NORE1A–Ras complex. (**A**) Ribbon representation of the overall Ras · GppNHp–NORE1A structure. The RBD of NORE1A is represented in green, and Ras is shown in blue. The Ras-bound nucleotide is shown in a ball-and-stick representation. The dashed connection between β_1 and β_2 of NORE1A indicates residues 249–273, which are not visible in the electron density. (**B**) Structural comparison of NORE1A with the RBDs of RalGDS (PDB: 1LXD) and Raf (PDB: 1GUA) depicted in red and yellow, respectively. The complex is rotated 180° with respect to (A). (**C**) Schematic drawing of the domain organization of NORE1A, RAPL and RASSF1A (C1, DAG binding domain; RBD, Ras binding domain; SARAH, Sav/RASSF/Hpo interaction domain). The cross-striped part or the RBDs indicate the size of the domains predicted by SMART. Dashed lines represent binding sites for microtubules (MT) and MST1/2. (**D**) Sequence alignment of the RBDs of all six members of the human RASSF. Secondary structure elements of NORE1A are indicated. To maintain the notation of the canonical RBD, we termed the helix and the strand within the unique N terminus as α_N and β_N. Residues of mouse NORE1A that differ from human orthologue are represented below the alignment. Positions that match conserved residues are highlighted in grey; residues involved in Ras binding are indicated by asterisks.

were 70- to 90-fold weakened compared with wt NORE1A. On the Ras side, the aromatic ring portion of Tyr64 in switch II is most relevant for NORE1A interaction by forming hydrophobic contacts to F234, C220 and L221 (Figure 3D and Supplementary Figure 2). We analysed the contribution of this side chain by mutating to Ala and observed a 94-fold weaker interaction with wt NORE1A. Considering 40.5 kJ/mol as the total change of free energy of NORE1A–Ras complex formation, deletion of this tyrosine side chain in switch II causes a major loss of 11.7 kJ/mol, indicating that Y64 contributes strongly to complex formation with NORE1A. To validate the specificity of this interaction, we used the RBD of Raf (residues 51–131) (Herrmann *et al*, 1995) as a control and determined the K_D value for the complex with the Ras Y64A mutant. We obtained a K_D value of 0.2 μM, which is similar to that of Raf-RBD and wt Ras (Wohlgemuth *et al*, 2005).

Probing the interaction of Ras and the RBD of RASSF1

RASSF1A is the closest NORE1A relative identified to date. Similar to NORE1A, the protein has been shown to colocalize on microtubules, to bind to the proapoptotic kinases MST1/2 and to be capable of interacting with the active form of Ras (Donninger *et al*, 2007). RASSF1A and NORE1A share the same domain architecture; both contain a C1 domain followed by an RBD and a SARAH domain at the C terminus (Figure 2C). A sequence alignment of all members of the RASSF reveals that RASSF1 is 53% identical to the RBD of

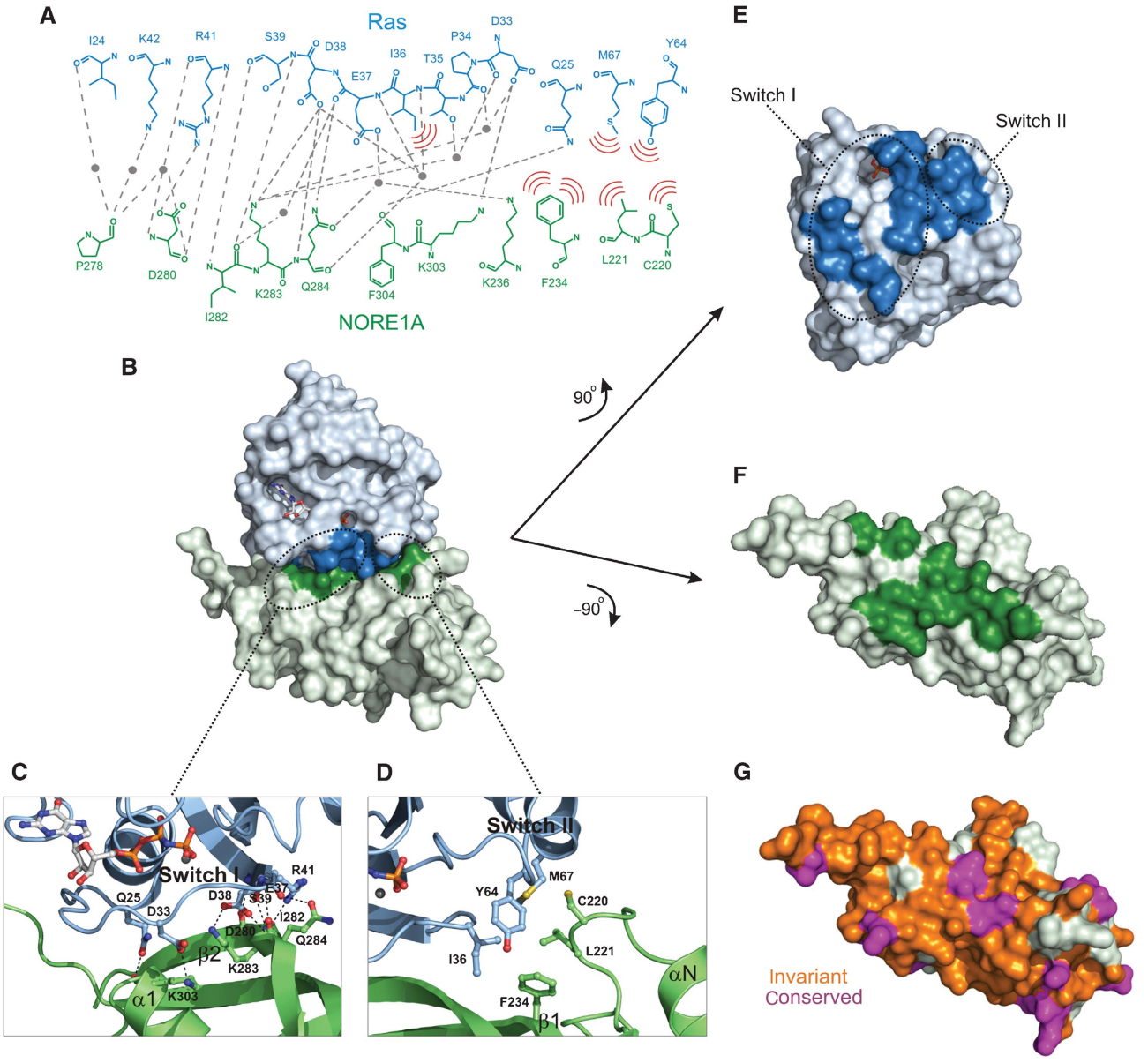

Figure 3 The NORE1A–Ras interface. (**A**) Schematic drawing of interacting residues in Ras (blue) and NORE1A (green). Hydrogen bonds (cutoff level 3.5 Å) are shown as dashed lines. Water molecules mediating polar interactions are displayed as dots. Hydrophobic interactions (cutoff level 4 Å) are shown as red lines. (**B**) Surface representation of the complex between Ras (pale blue) and NORE1A (pale green). Residues of the interface area are shown in bright blue or green. (**C**) Close-up view of the switch I interface. Residues forming polar contacts are shown as ball and sticks. Water molecules are omitted for clarity. (**D**) Close-up view of the switch II interface. Residues forming hydrophobic interactions are indicated. (**E**) Surface representation of Ras. The molecule is rotated by 90° with respect to (B) to visualize the interface areas (bright blue). The switch I and II regions are indicated. (**F**) Surface representation of NORE1A. The protein is rotated by −90°. The interface area is represented in bright green. (**G**) NORE1A structure in the same orientation as in (F) coloured according to sequence conservation.

NORE1A, the highest value among all RASSF proteins (Figure 2D). The projection of conserved residues onto the surface of the RBD of NORE1A suggests a similar mode of interaction between RASSF1A and Ras (Figure 3G). To prove this hypothesis, we purified the fragment 133–291 of RASSF1A, which corresponds to the RBD of NORE1A. Using the GDI assay we obtained a K_D value of 2.7 μM for the interaction between Ras and RASSF1A (Figure 4C), meaning that this interaction is 33 times weaker than the interaction between NORE1A and Ras. However, it is in the same range as observed for Rap1/NORE1A or Ras/RalGDS, indicating that residues 133–291 of RASSF1A in fact represent its RBD.

Kinetic analysis of NORE1A–Ras complex formation

The interface of the NORE1A–Ras complex buries a total surface of 1546 $Å^2$ (calculated with CNS using a probe of 1.5 Å), which is significantly enlarged compared with other Ras effector complexes such as Raf-RBD (1333 $Å^2$) (Nassar *et al*, 1996) or RalGDS-RBD (1331 $Å^2$) (Vetter *et al*, 1999) (Figure 3E and F). To find out if and how this extension influences the dynamics of complex formation, we performed stopped-flow measurements to evaluate the kinetics of the NORE1A–Ras interaction (Figure 5). We obtained an association rate constant for NORE1A and Ras of 11.9 $\mu M^{-1} s^{-1}$. In contrast to the Ras–Raf complex, which has a higher association rate constant of 66 $\mu M^{-1} s^{-1}$ indicating a high-affinity

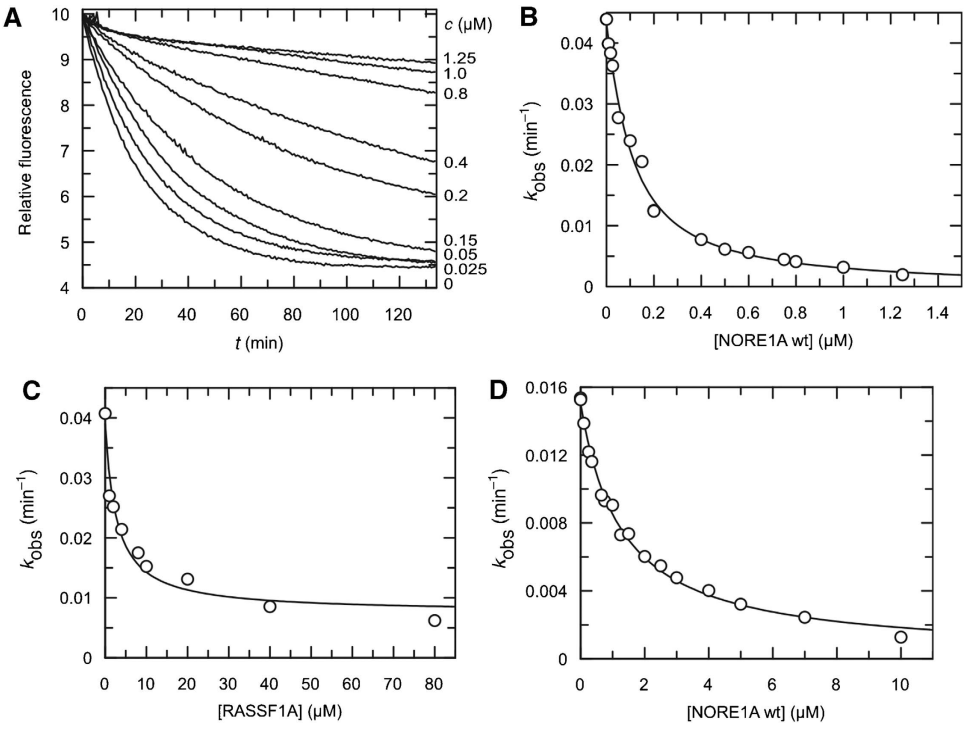

Figure 4 GDI assay with NORE1A and RASSF1A. (**A**) Time course of the fluorescence decay given in relative units when excess of unlabelled nucleotide is added to solutions of Ras-mantGppNHp and NORE1A-RBD at different concentrations. (**B**) Rate constants for the nucleotide dissociation from Ras, obtained from the experiment in (A), are plotted versus the concentration of the NORE1A-RBD. A quadratic binding curve fitted to the data yield the K_D value for Ras–NORE1A interaction of 0.8 μM. The same experiments were performed to probe the interaction between Ras and RASSF1A-RBD (**C**) or Rap1 and NORE1A (**D**) resulting in K_D values of 2.7 and 1.3 μM, respectively.

Table II Equilibrium dissociation constants (K_D values) for complexes between NORE1A and Ras and Rap mutants

	NORE1A wt		NORE1A K302D	
	K_D (μM)	K_D (mut)/K_D (wt)	K_D (μM)	K_D (mut)/K_D (wt)
Ras				
wt	0.08	—	0.71	9
D30E/E31K	1.23	15	0.77	0.1
Y64A	7.5	94	—	—
Rap1A				
wt	1.3	—	0.7	0.55
E30D/K31E	0.17	0.13	1.1	6.6

Table III Equilibrium dissociation constants (K_D values) for complexes between Ras and NORE1A mutants and RASSF1

	Ras (wt)	
	K_D (μM)	K_D (mut)/K_D (wt)
NORE1		
wt	0.08	—
C220A	0.48	6.0
C220D	5.7	71
L221A	1.7	21
L221D	7.5	93
F234A	0.55	6.9
K236A	0.41	5
D280A	0.17	2.1
K283A	19.1	240
Q284A	0.15	1.9
K303A	3.5	43
Δloop (255–274)	0.07	0.9
RASSF1	2.7	—

interaction, the k_{on} value found for NORE1A is in a similar range as the weak Ras binders such as RalGDS and PI3K. However, we observed a dissociation rate constant, k_{off}, of 0.1 s^{-1} for NORE1A-RBD, which is much slower compared with all other Ras effectors and which is responsible for the tight interaction of the complex. The reciprocal of the dissociation rate constant is the average lifetime of the complex, which is in the range of 60–250 ms for Ras/PI3K, Ras/RalGDS and Ras/Raf (Herrmann, 2003). In contrast, NORE1A remains in a Ras-bound complex, with an average lifetime of 10 s. This prolonged duration must be a consequence of the enlargement of interface, which is caused by the elongated strands β_1 and β_2 in switch I and the unique switch II binding site. To evaluate the significance of the additional switch II binding sites for slow complex dissociation, we analysed the dynamics of mutants within the switch II interface of the Ras–NORE1A complex. As shown in Figure 5, the dissociation kinetics for C220A, L221A and F234A NORE1A mutants individually revealed a 4- to 30-fold accelerated dissociation compared with that for wt whereas the k_{on} values were only two times smaller. Even more pronounced were the increases in k_{off} values for the aspartate mutants (Table IV). A similar result was obtained for the dissociation of wt and RasY64A mutant NORE1A with a 150-fold increase in k_{off}. These results

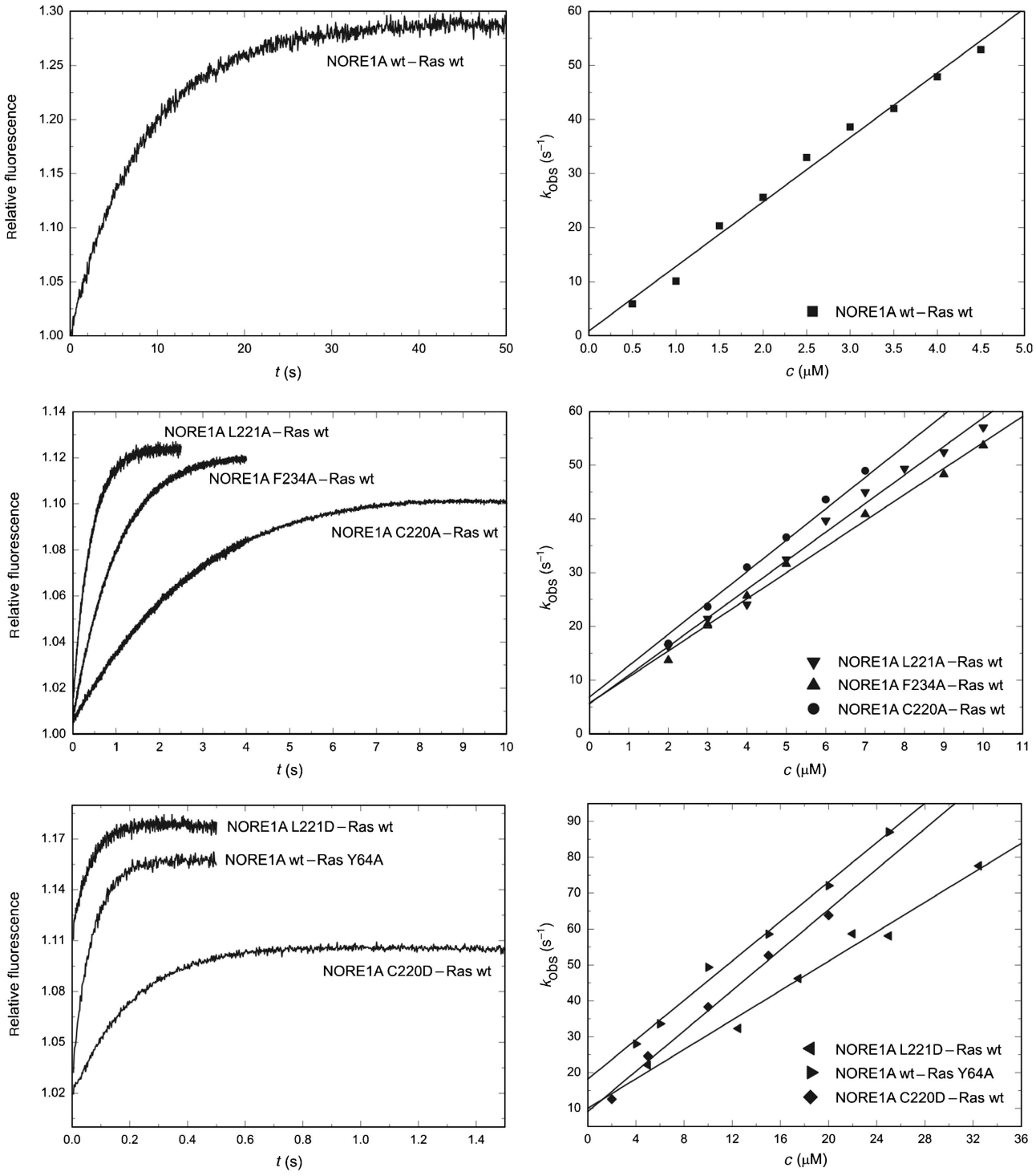

Figure 5 Impact of the hydrophobic contact area onto the dynamics of the NORE1A–Ras interaction. Left panel: Dissociation rate constants k_{off} for the wt and mutant NORE1A–Ras · mGppNHp complex were determined by stopped-flow measurements using an excess of unlabelled Ras · GppNHp for displacement. A single exponential equation was fitted to the observed fluorescence change to obtain k_{off}. Right panel: Stopped-flow measurements were performed using pseudo-first-order conditions to determine association rate constants k_{on} of wt and mutant Ras or NORE1A proteins. The observed association rate constants k_{obs} were plotted against wt or mutant NORE1A concentration to obtain k_{on} by linear fitting.

indicate that the switch II interface contributes to a prolonged lifetime of the Ras–NORE1A complex.

Discussion

NORE1A, a founding member of the RASSF family, is the first Ras effector with non-enzymatic function for which the three-dimensional structure of the RBD has been characterized. NORE1A acts as a scaffold for the proapoptotic kinase MST1; it is believed that NORE1A forms a complex with inactive MST1, which can be activated on binding of NORE1A to Ras (Praskova *et al*, 2004). Similar to other RASSF proteins, NORE1A localizes to microtubules and centrosomes, a feature that seems to be important for the

growth and tumour suppressive properties of the RASSF. The molecular mechanism by which RASSF proteins induce growth and tumour suppression is not known in detail. However, one can hypothesize that at least some of these activities are regulated by the small GTPase Ras, as bioinformatics analysis predicts an RA domain in all six members of the RASSF (Schultz *et al*, 1998). At least for NORE1A, it has been shown that Ras binding is required for growth suppressive activities (Moshnikova *et al*, 2006).

The RA domains are predicted to consist of about 90 residues in the C-terminal half of the RASSF proteins. These predictions have been widely accepted, as can be seen by several publications addressing the RASSF. Therefore, it was a surprise to discover the true RBD of NORE1A to comprise 160 residues, which is twice as large as the Raf-RBD. Despite this remarkable size, the overall architecture follows a ubiquitin fold, which is the common topology of RBDs. The enlargement can be ascribed to (i) a loop insertion between residues 249 and 273 (between β_1 and β_2), (ii) an extension of the β_1/β_2 sheet and (iii) an additional subdomain at the N terminus of the RBD consisting of a short β-strand and an α-helix. The flexible loop between β_1 and β_2 can be deleted without impairing the interaction with Ras. It can only be speculated about its role in the interaction with other NORE1A partners or with other domains of NORE1A such as the C1 domain, which has been shown to form an intramolecular complex with the RBD (Harjes *et al*, 2006). Recently, it has been reported that RASSF1A is phosphorylated at T202 and S203 by the mitotic kinase Aurora-A and this phosphorylation prevents RASSF1A interaction with microtubules (Rong *et al*, 2007). These two phosphorylation sites are highly conserved among the members of the RASSF. T202/S203 in RASSF1A corresponds to position T274/S275 in NORE1A and is located just before strand β_2, at the end of the loop insertion. Thus, it might be possible that the loop insertion serves as an interacting element for kinases such as Aurora-A.

In contrast to the loop insertion, the N-terminal subdomain establishes a hydrophobic interface with Ras switch II and thus is important in the interaction with Ras. The 30 amino acids that form the subdomain are indispensable for Ras binding in HEK293 cells. As described, any mutation within the hydrophobic framework leads to a dramatic loss of binding energy and disrupts the interaction with Ras. In contrast to other effectors such as Raf, the mutation Y64A in Ras switch II does perturb binding to NORE1A, which underlines the specific interaction between Ras switch II and NORE1A. Interestingly, it has been reported that Y64 in switch II of Ras is also involved in the binding of PI3K and PLCε (Pacold *et al*, 2000; Bunney *et al*, 2006). Both RBDs exhibit a phenylalanine residue in strand β_1, which interacts with Y64 of switch II similar to F234 in NORE1A (Figure 6A). This indicates that a hydrophobic interaction between Y64 in Ras and a phenylalanine residue in strand β_1 of the canonical ubiquitin cores might be conserved among some RBDs. However, we could not find any other example for an extended switch II interface formed by an N-terminal helical subdomain as observed in the NORE1A–Ras structure. The functional consequences of the unique switch II interface were revealed by kinetic studies. The average lifetime of the Ras–NORE1A complex is as long as 10 s, which is at least an order of magnitude longer compared to any Ras effector characterized so far. Disruption of the unique switch II binding interface by mutation leads to rate constants, and hence lifetimes, similar to those of the short-lived complexes formed between Ras and effectors such as Raf, RalGDS or

Table IV Association and dissociation rate constants (k_{on} and k_{off} values, respectively) and average lifetimes (τ values) for Ras/NORE1A complexes

NORE1/Ras	k_{on} ($\mu M^{-1} s^{-1}$)	k_{off} (s^{-1})	τ (s)
wt/wt	11.9	0.1	10
C220A/wt	6.4	1.0	1.0
C220D/wt	2.6	5.1	0.2
L221A/wt	5.7	2.5	0.4
L221D/wt	2.7	16.9	0.06
F234A/wt	4.8	0.3	3.3
wt/Y64A	1.5	14.9	0.07

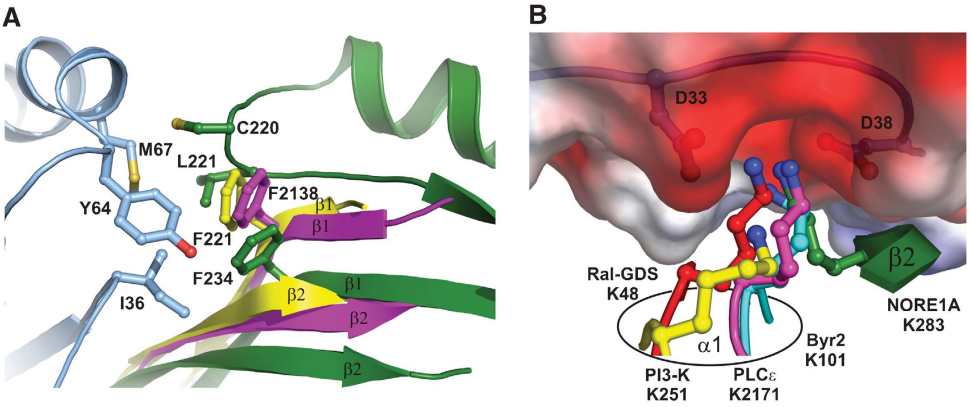

Figure 6 Structural comparison of different effectors in complex with Ras. (**A**) The interaction between Y64 in Ras (blue) and the phenylalanine of strand β_1 in NORE1A (green), PI3K (PDB: 1HE8) (yellow) or PLCε (PDB: 2C5L) (magenta) shows a similar spatial arrangement. The relative displacement of the β-sheet in NORE1A allows participation of C220 and L221 in Ras switch II interaction. (**B**) Spatial comparison of lysine residues in helix α1 of the effectors RalGDS, PI3K, PLCε, Byr2 (PDB: 1K8R) and in strand β_2 of NORE1A, which participate in Ras binding by fitting into a negatively charged groove formed by D33 and D38 of switch I. The molecules were superimposed by the least square fit procedure using the program Xfit.

PI3K, which are in the range of 60–250 ms (Sydor *et al*, 1998; Pacold *et al*, 2000; Linnemann *et al*, 2002; Kiel *et al*, 2004). A distinctive lifetime of a Ras/effector complex might be related to the functional role of the effector. Raf, PI3K, etc. bear direct catalytic activity, whereas the RASSF proteins such as NORE1A do not have any enzymatic function. Rather, NORE1A acts as a scaffold protein for other molecules. Therefore, it might be favourable for an adaptor protein such as NORE1A to remain in complex with Ras for a longer duration to facilitate activation of its binding partners such as MST1/2.

Our biochemical data demonstrate how molecular recognition and discrimination between Ras and Rap by NORE1A is substantiated (Supplementary Figure 3). Lysine 302 in helix α_1 most likely forms a salt bridge with glutamate 31 in switch I of Ras. In Rap1, the corresponding amino acid is K31. This charge reversal results in a 15-fold reduced affinity to NORE1A as determined by GDI assay using wt Rap1 and the Rap homologue Ras(D30E/E31K) mutant. Strikingly, the Ras homologue Rap(E30D/K31E) mutant increases the affinity to NORE1A seven-fold compared with wt Rap1, indicating clearly that restoration of the salt bridge established between aspartate in Ras and lysine in NORE1A is responsible for the binding preference of NORE1A to Ras. As shown in earlier studies, specificity of complex formation between Raf-RBD and Ras or Rap1 is similarly determined by lysine at position 84 in helix α1 of Raf and at position 31 in Ras and Rap1, respectively (Nassar *et al*, 1996). Thus, the opposite/equal charge of these amino-acid pairs generally seems to define specificity in Ras/Rap1 effectors interaction.

Owing to a structurally conserved set of positively charged residues within the RBDs and the predominantly acidic switch I region of Ras, all Ras/effector complexes show a polar interface with high charge complementarities of the two sides. Similar to other Ras effectors, NORE1A exhibits a pattern of three positively charged key residues where K283 is the most important one, as evident from the 240-fold increase in the K_D value after deletion of the lysine side chain. The lysine residue points into an acidic groove of the Ras interface, which is constituted by the two aspartate residues 33 and 38. A similar interaction pattern can be observed in other structures of Ras in complex with RalGDS (Vetter *et al*, 1999), PI3K (Pacold *et al*, 2000), PLCε (Bunney *et al*, 2006) or Byr2 (Scheffzek *et al*, 2001) (Figure 6B). Corresponding alanine mutations of these effectors result in a comparable drastic loss of Ras affinity. Interestingly, the lysine side chain of NORE1A originates from β_2 in contrast to all other Ras effectors in which the lysine residues are located in α_1. This observation demonstrates a notable variation of a conserved interaction pattern. The saturation of the negative binding epitope formed by Asp33 and Asp38 in Ras by a lysine positive charge on the effector side seems to be necessary for a strong interaction.

As RAPL/NORE1B is a splice variant of NORE1A possessing the same RBD, the structural and biochemical data reported here apply to RAPL as well (Figure 2C). Likewise, owing to the high homology within the RASSF, the structure of NORE1A is also of importance for other RASSF proteins, in particular for RASSF1A (Figures 2D and 3G). Close homology of NORE1A to RASSF1A suggests a similar structural arrangement; the interaction of RASSF1A with Ras, although weaker than NORE1A/Ras interaction, has been demonstrated in this study.

As mentioned above, one of the main functions of RASSF proteins is related to their association with the microtubule cytoskeleton, which has been shown to be crucial for their tumour suppressor properties. Most intriguingly, the tubulin binding region was mapped by cell biological experiments exactly to the RBD that we have characterized here (Moshnikova *et al*, 2006) (Figure 2C). Therefore, it will be interesting to investigate the functional role of Ras or Rap1 in the interplay between tubulin and RASSF proteins. The structure of the RASSF tumour suppressor family member NORE1A in complex with Ras, which we have presented in this report, should be a vantage point.

Materials and methods

Expression, purification and mutagenesis

Murine NORE1A (200–358) was expressed as a GST fusion protein in BL21 cells. Purification details are described elsewhere (Wohlgemuth *et al*, 2005). Human NORE1A (202–361 and the deletion mutant) was synthesized and purified in the same way. H-Ras (1–166) and Rap1A (1–167) were prepared from *Escherichia coli* strain CK600K using the *ptac* expression system and loaded with either GppNHp or mantGppNHp using alkaline phosphatase as described previously (Herrmann *et al*, 1996). Plasmids encoding FLAG or haemagglutinin (HA) epitope-tagged proteins for expression in HEK293 cells have been described previously (Khokhlatchev *et al*, 2002) or prepared using the standard molecular biology techniques (Sambrook and Russel, 2001). Mutants were generated using the Quickchange site directed mutagenesis kit (Stratagene) and verified by sequencing.

Crystallography

Crystals of NORE1A L285M/K302D (amino acids 200–358) in complex with Ras·GppNHp D30E/E31K (amino acids 1–166) were grown at 293 K in hanging drop set-ups using a reservoir solution containing 100 mM sodium acetate, 20% PEG 2000, 250 mM $(NH_4)_2SO_4$, 10 mM DTE and 10 mg/ml protein. The L285M mutation was primary introduced for selenomethionine labelling. Crystals were flash-frozen in liquid nitrogen with a solution containing the mother liquor and 7.5% sucrose. Data were collected at 100 K. Crystals diffract to 1.8 Å resolution and belong to the monoclinic space group C2 with one molecule per asymmetric unit. A data set of high redundancy was collected at beamline ID14-4 of ESRF and processed with XDS (Kabsch, 1988). Structure determination was performed with the molecular replacement method by using the refined coordinates of Ras·GppNHp (PDB code 5P21) as the starting model in rotation and translation search calculations carried out using AMoRe, CCP4 (Bailey, 1994). An initial map calculated with the phases of the search model showed a clear electron density for most of the RBD of NORE1A. The model of the Ras·GppNHp–NORE1A complex was automatically constructed using ARP/wARP (Perrakis *et al*, 2001) and subjected to iterative rounds of model improvement and refinement. The program Xfit (McRee, 1999) was used to build the final model into $2F_o-F_c$ and F_o-F_c maps, and refinement was carried out with REFMAC (Murshudov *et al*, 1997). Composite simulated annealing maps calculated with CNS (Brunger *et al*, 1998) were regularly used to avoid model bias. The final model exhibits good stereochemistry as judged by the program Procheck (Laskowski *et al*, 1993) and consists of 298 amino acids, 115 water molecules, one GppNHp and one magnesium ion. Residues 249–273 are not visible in the electron density due to conformational flexibility. Figures were generated using PyMol (DeLano, 2002).

Biochemistry

The affinities between NORE1A and Ras were quantified by taking advantage of the GDI effect of effector binding as observed for other Ras effector proteins (Herrmann *et al*, 1996). The time course of the mant-nucleotide dissociation was recorded by a spectrofluorimeter (LS-55, Perkin-Elmer) at 37°C using 50 nM Ras·mGppNHp,

different concentrations of NORE1A-RBD and a 1000-fold excess of unlabelled GppNHp. All measurements were performed in buffer PX (50 mM Tris buffer (pH 7.4) containing 5 mM $MgCl_2$ and 2 mM DTE). The K_D values were determined from the concentration dependence of the observed rate constants as described previously (Herrmann *et al*, 1996).

Stopped-flow measurements were made at 10°C in buffer PX using an SFM-400 apparatus (Biologic). A 0.6 μM portion of Ras bound to mGppNHp was mixed with increasing concentrations of NORE1A-RBD. For dissociation kinetics, the preincubated NORE1A–Ras · mGppNHp complex was rapidly mixed with a 60-fold excess of Ras · GppNHp for displacement. Fluorescence was excited at 360 nm and recorded through a 420 nm cutoff filter. The experimental errors on the values obtained, rate constants and K_D values are in the range of 10–20%.

HEK293 cells (ATCC, Manassas, VA) were cultivated and transfected using the Lipofectamine reagent as described previously (Khokhlatchev *et al*, 2002) and harvested 48 h after transfection. Anti-FLAG antibody was from Sigma Chemical Company (St Louis, MO), and anti-HA was from CRP Inc. (Berkeley, CA). For the detection of NORE1A-Ras association, frozen cells were scraped into filtered lysis buffer A (30 mM HEPES (pH 7.4), 1% (w/v) Triton X-100, 20 mM β-glycerophosphate, 1 mM orthovanadate, 20 mM NaF, 20 mM KCl, 2 mM EGTA, 7.5 mM $MgCl_2$, 14 mM β-mercaptoethanol and a protease inhibitor cocktail (Sigma)). Lysates were centrifuged at 17 000 *g* for 40 min. Supernatants were mixed with anti-HA antibodies and incubated at 4°C for 1.5–2 h. Protein A/G–Sepharose (Pierce Biotechnology Inc., Rockford, IL) was added thereafter for an additional 1.5 h. Beads were extensively washed in lysis buffer and eluted directly onto SDS sample buffer. Extracted proteins were separated by SDS–PAGE, transferred onto PVDF membranes and probed with the antibodies indicated. Bound antibodies were visualized with ECL (Pierce).

Supplementary data

Supplementary data are available at *The EMBO Journal* Online (http://www.embojournal.org).

Acknowledgements

We thank I Schlichting and W Blankenfeld for data collection. We gratefully acknowledge Deutsche Forschungsgemeinschaft (SFB 642), Studienstiftung des deutschen Volkes and Wendy Will Case Cancer Fund for financial support.

The atomic coordinates of the Ras–NORE1A complex have been deposited in the Protein Data Bank with the accession number 3DDC. The authors declare no competing financial interests.

References

Agathanggelou A, Cooper WN, Latif F (2005) Role of the Ras-association domain family 1 tumor suppressor gene in human cancers. *Cancer Res* **65:** 3497–3508

Aoyama Y, Avruch J, Zhang XF (2004) Norel inhibits tumor cell growth independent of Ras or the MST1/2 kinases. *Oncogene* **23:** 3426–3433

Bailey S (1994) The CCP4 suite: programs for protein crystallography. *Acta Crystallogr D Biol Crystallogr* **50:** 760–763

Baksh S, Tommasi S, Fenton S, Yu VC, Martins LM, Pfeifer GP, Latif F, Downward J, Neel BG (2005) The tumor suppressor RASSF1A and MAP-1 link death receptor signaling to Bax conformational change and cell death. *Mol Cell* **18:** 637–650

Brunger AT, Adams PD, Clore GM, DeLano WL, Gros P, Grosse-Kunstleve RW, Jiang JS, Kuszewski J, Nilges M, Pannu NS, Read RJ, Rice LM, Simonson T, Warren GL (1998) Crystallography & NMR system: a new software suite for macromolecular structure determination. *Acta Crystallogr D Biol Crystallogr* **54:** 905–921

Bunney TD, Harris R, Gandarillas NL, Josephs MB, Roe SM, Sorli SC, Paterson HF, Rodrigues-Lima F, Esposito D, Ponting CP, Gierschik P, Pearl LH, Driscoll PC, Katan M (2006) Structural and mechanistic insights into ras association domains of phospholipase C epsilon. *Mol Cell* **21:** 495–507

Dammann R, Li C, Yoon JH, Chin PL, Bates S, Pfeifer GP (2000) Epigenetic inactivation of a RAS association domain family protein from the lung tumour suppressor locus 3p21.3. *Nat Genet* **25:** 315–319

Dammann R, Schagdarsurengin U, Strunnikova M, Rastetter M, Seidel C, Liu L, Tommasi S, Pfeifer GP (2003) Epigenetic inactivation of the Ras-association domain family 1 (RASSF1A) gene and its function in human carcinogenesis. *Histol Histopathol* **18:** 665–677

DeLano WL (2002) The PyMOL Molecular Graphics System on World Wide http://www.pymol.org

Donninger H, Vos MD, Clark GJ (2007) The RASSF1A tumor suppressor. *J Cell Sci* **120:** 3163–3172

Harjes E, Harjes S, Wohlgemuth S, Muller KH, Krieger E, Herrmann C, Bayer P (2006) GTP-Ras disrupts the intramolecular complex of C1 and RA domains of Nore1. *Structure* **14:** 881–888

Herrmann C (2003) Ras-effector interactions: after one decade. *Curr Opin Struct Biol* **13:** 122–129

Herrmann C, Horn G, Spaargaren M, Wittinghofer A (1996) Differential interaction of the ras family GTP-binding proteins H-Ras, Rap1A, and R-Ras with the putative effector molecules Raf kinase and Ral-guanine nucleotide exchange factor. *J Biol Chem* **271:** 6794–6800

Herrmann C, Martin GA, Wittinghofer A (1995) Quantitative analysis of the complex between p21ras and the Ras-binding domain of the human Raf-1 protein kinase. *J Biol Chem* **270:** 2901–2905

Kabsch W (1988) Automatic indexing of rotation diffraction patterns. *J Appl Crystallogr* **21:** 67–72

Katagiri K, Maeda A, Shimonaka M, Kinashi T (2003) RAPL, a Rap1-binding molecule that mediates Rap1-induced adhesion through spatial regulation of LFA-1. *Nat Immunol* **4:** 741–748

Khokhlatchev A, Rabizadeh S, Xavier R, Nedwidek M, Chen T, Zhang XF, Seed B, Avruch J (2002) Identification of a novel Ras-regulated proapoptotic pathway. *Curr Biol* **12:** 253–265

Kiel C, Selzer T, Shaul Y, Schreiber G, Herrmann C (2004) Design of faster Ras-binding Ral guanine dissociation stimulator mutants: electrostatic steering affects the rate of association by increasing the stability of the encounter complex. *Proc Natl Acad Sci USA* **101:** 19223–19228

Kinashi T, Katagiri K (2004) Regulation of lymphocyte adhesion and migration by the small GTPase Rap1 and its effector molecule, RAPL. *Immunol Lett* **93:** 1–5

Laskowski RA, MacArthur MW, Moss DS, Thornton JM (1993) PROCHECK: a program to check the stereochemical quality of protein structures. *J Appl Crystallogr* **26:** 283–291

Letunic I, Copley RR, Pils B, Pinkert S, Schultz J, Bork P (2006) SMART 5: domains in the context of genomes and networks. *Nucleic Acids Res* **34:** D257–D260

Linnemann T, Kiel C, Herter P, Herrmann C (2002) The activation of RalGDS can be achieved independently of its Ras binding domain. Implications of an activation mechanism in Ras effector specificity and signal distribution. *J Biol Chem* **277:** 7831–7837

Liu L, Tommasi S, Lee DH, Dammann R, Pfeifer GP (2003) Control of microtubule stability by the RASSF1A tumor suppressor. *Oncogene* **22:** 8125–8136

Liu L, Vo A, McKeehan WL (2005) Specificity of the methylation-suppressed A isoform of candidate tumor suppressor RASSF1 for microtubule hyperstabilization is determined by cell death inducer C19ORF5. *Cancer Res* **65:** 1830–1838

Malumbres M, Barbacid M (2003) RAS oncogenes: the first 30 years. *Nat Rev Cancer* **3:** 459–465

McRee DE (1999) XtalView/Xfit—a versatile program for manipulating atomic coordinates and electron density. *J Struct Biol* **125:** 156–165

Miertzschke M, Stanley P, Bunney TD, Rodrigues-Lima F, Hogg N, Katan M (2007) Characterization of interactions of adapter protein RAPL/Nore1B with RAP GTPases and their role in T cell migration. *J Biol Chem* **282:** 30629–30642

Moshnikova A, Frye J, Shay JW, Minna JD, Khokhlatchev AV (2006) The growth and tumor suppressor NORE1A is a cytoskeletal protein that suppresses growth by inhibition of the ERK pathway. *J Biol Chem* **281:** 8143–8152

Murshudov GN, Vagin AA, Dodson EJ (1997) Refinement of macromolecular structures by the maximum-likelihood method. *Acta Crystallogr D Biol Crystallogr* **53:** 240–255

Nassar N, Horn G, Herrmann C, Block C, Janknecht R, Wittinghofer A (1996) Ras/Rap effector specificity determined by charge reversal. *Nat Struct Biol* **3:** 723–729

Oh HJ, Lee KK, Song SJ, Jin MS, Song MS, Lee JH, Im CR, Lee JO, Yonehara S, Lim DS (2006) Role of the tumor suppressor RASSF1A in Mst1-mediated apoptosis. *Cancer Res* **66:** 2562–2569

Pacold ME, Suire S, Perisic O, Lara-Gonzalez S, Davis CT, Walker EH, Hawkins PT, Stephens L, Eccleston JF, Williams RL (2000) Crystal structure and functional analysis of Ras binding to its effector phosphoinositide 3-kinase gamma. *Cell* **103:** 931–943

Perrakis A, Harkiolaki M, Wilson KS, Lamzin VS (2001) ARP/wARP and molecular replacement. *Acta Crystallogr D Biol Crystallogr* **57:** 1445–1450

Pfeifer GP, Yoon JH, Liu L, Tommasi S, Wilczynski SP, Dammann R (2002) Methylation of the RASSF1A gene in human cancers. *Biol Chem* **383:** 907–914

Praskova M, Khoklatchev A, Ortiz-Vega S, Avruch J (2004) Regulation of the MST1 kinase by autophosphorylation, by the growth inhibitory proteins, RASSF1 and NORE1, and by Ras. *Biochem J* **381:** 453–462

Price LS, Bos JL (2004) RAPL: taking the Rap in immunity. *Nat Immunol* **5:** 1007–1008

Rong R, Jiang LY, Sheikh MS, Huang Y (2007) Mitotic kinase Aurora-A phosphorylates RASSF1A and modulates RASSF1A-mediated microtubule interaction and M-phase cell cycle regulation. *Oncogene* **26:** 7700–7708

Sambrook J, Russel DW (2001) *Molecular Cloning: A Laboratory Manual*. New York: Cold Spring Harbor Laboratory Press

Scheel H, Hofmann K (2003) A novel interaction motif, SARAH, connects three classes of tumor suppressor. *Curr Biol* **13:** R899–R900

Scheffzek K, Grunewald P, Wohlgemuth S, Kabsch W, Tu H, Wigler M, Wittinghofer A, Herrmann C (2001) The Ras–Byr2RBD complex: structural basis for Ras effector recognition in yeast. *Structure* **9:** 1043–1050

Schultz J, Milpetz F, Bork P, Ponting CP (1998) SMART, a simple modular architecture research tool: identification of signaling domains. *Proc Natl Acad Sci USA* **95:** 5857–5864

Sydor JR, Engelhard M, Wittinghofer A, Goody RS, Herrmann C (1998) Transient kinetic studies on the interaction of Ras and the Ras-binding domain of c-Raf-1 reveal rapid equilibration of the complex. *Biochemistry* **37:** 14292–14299

Terada T, Ito Y, Shirouzu M, Tateno M, Hashimoto K, Kigawa T, Ebisuzaki T, Takio K, Shibata T, Yokoyama S, Smith BO, Laue ED, Cooper JA (1999) Nuclear magnetic resonance and molecular dynamics studies on the interactions of the Ras-binding domain of Raf-1 with wild type and mutant Ras proteins. *J Mol Biol* **286:** 219–232

van der Weyden L, Adams DJ (2007) The Ras-association domain family (RASSF) members and their role in human tumourigenesis. *Biochim Biophys Acta* **1776:** 58–85

Vavvas D, Li X, Avruch J, Zhang XF (1998) Identification of Nore1 as a potential Ras effector. *J Biol Chem* **273:** 5439–5442

Vetter IR, Linnemann T, Wohlgemuth S, Geyer M, Kalbitzer HR, Herrmann C, Wittinghofer A (1999) Structural and biochemical analysis of Ras-effector signaling via RalGDS. *FEBS Lett* **451:** 175–180

Vetter IR, Wittinghofer A (2001) The guanine nucleotide-binding switch in three dimensions. *Science* **294:** 1299–1304

Vos MD, Dallol A, Eckfeld K, Allen NP, Donninger H, Hesson LB, Calvisi D, Latif F, Clark GJ (2006) The RASSF1A tumor suppressor activates Bax via MOAP-1. *J Biol Chem* **281:** 4557–4563

Vos MD, Martinez A, Ellis CA, Vallecorsa T, Clark GJ (2003) The pro-apoptotic Ras effector Nore1 may serve as a Ras-regulated tumor suppressor in the lung. *J Biol Chem* **278:** 21938–21943

Wohlgemuth S, Kiel C, Kramer A, Serrano L, Wittinghofer F, Herrmann C (2005) Recognizing and defining true Ras binding domains. I: biochemical analysis. *J Mol Biol* **348:** 741–758